

# Wave Function Based Characteristics of Hybrid Mesons

Nosheen Akbar\* , Bilal Masud† , Saba Noor‡

*Centre For High Energy Physics, University of the Punjab, Lahore(54590), Pakistan.*

## Abstract

We propose some extensions of the quark potential model to hybrids, fit them to the lattice data and use them for the purpose of calculating the masses, root mean square radii and wave functions at the origin of the conventional and hybrid charmonium mesons. We treat the ground and excited gluonic field between a quark and an antiquark as in the Born-Oppenheimer expansion, and use the shooting method to numerically solve the required Schrödinger equation for the radial wave functions; from these wave functions we calculate the mesonic properties. For masses we also check through a Crank Nicholson discretization. For hybrid charmonium mesons, we consider the exotic quantum number states with  $J^{PC} = 0^{+-}, 1^{-+}$  and  $2^{+-}$ . We also compare our results with the experimentally observed masses and theoretically predicted results of the other models. Our results have implications for scalar form factors, energy shifts, magnetic polarizabilities, decay constants, decay widths and differential cross sections of conventional and hybrid mesons.

## I. Introduction

A number of hadron properties are well described by the quark model where mesons have quantum numbers  $J = L \oplus S$ ,  $P = (-1)^{L+1}$  and  $C = (-1)^{L+S}$ ,  $L$  and  $S$  being the quantum numbers for the quark-antiquark orbital angular momentum and their net spin angular momentum respectively. The states with  $J^{PC} = 0^{+-}, 1^{-+}, 2^{+-}$  (for the lowest lying hybrids in the flux tube model) can not be formed from a  $q\bar{q}$  pair and hence are not allowed in the quark model. These states are signals for exotic mesons (hybrids, glueballs, etc). Quantum Chromodynamics (QCD), describing the interaction between quarks and gluonic field, predicts the existence of hybrid mesons containing the excited gluonic field. Thus for understanding of QCD, we need to find experimentally testable predictions of the theory for situations in which the gluonic field between a quark and antiquark is in an excited state. Thus hybrids are an important source of information related to confining properties of QCD, and checking for existence of hybrid mesons is very important objective of particle physics. Reviews of the spectrum of excited gluonic states can be found in ref. [1]. Recently, a resonance is observed at COMPASS [2] with  $J^{PC} = 1^{-+}$ . Some other groups like VES [3]-[5], E852 [6]-[10], and the Crystal Barrel collaboration [11] also observed these states.

Using the Born-Oppenheimer approach, the work of finding implications of QCD for a meson can be split into first using the numerical lattice simulations of QCD to fit parameters of a quark antiquark potential and then using this potential to calculate its dynamical implications. Even a numerically defined potential can be used in this scheme, as in refs. [12] [13]. These works use some potentials to calculate hybrid masses and few radial probability graphs (but presents no  $q\bar{q}$  wave function expressions or uses.). What we add to this work is that now we suggest a number of analytical expressions for the excited state gluonic field potential between a quark and antiquark and fit their parameters to the lattice data for the ground and excited state gluonic field energy values available in ref. [12] for discrete quark antiquark separations. For each case, we report a dimensionless chisquare and other measures directly telling how much fractional error each model has in fitting. We use this variety of potentials to indicate suitable ones for different applications, for example for analytical calculations of expectation values in few-body wave functions where a numerical approach may have convergence problems. Our full list of chisquare and other error measures tells how much extra error is generated in preferring the flux tube model and other integrable forms over the ones that can be only numerically used but fit better. After using these

---

\*e mail: noshinakbar@yahoo.com

†e mail: bilalmasud.chep@pu.edu.pk

‡e mail: sabanoor87@gmail.com

potentials to find the quark-antiquark wave functions, we also calculate a number of conventional and hybrid meson rms radii and square of radial wave functions at the origin. We continue till writing some implications of these for scalar form factors, energy shifts, magnetic polarizabilities, decay constants, decay widths and differential cross sections of conventional and hybrid mesons. All this is addition to our own results for meson masses and radial probabilities that are in agreement to those reported in ref. [12] for the height of the single peak of the probability graph.

In the present paper, we apply our techniques to charmonium mesons. An advantage of considering them is indicated in ref. [14] as

“ The best systems for a hybrid search may be  $c\bar{c}$  or  $b\bar{b}$  where there is a large gap between the lowest states and the  $D\bar{D}$  and  $B\bar{B}$  threshold respectively.”

To find the wave functions of conventional charmonium mesons, we use the realistic coulombic plus linear potential model to solve the Schrödinger equation numerically by using the corresponding quantum numbers of mesons. To study hybrids, we repeat the numerical work with the models of the gluonic excitation energy mentioned in section III. From the numerically found wave functions, we calculate the root mean square radii. These radii can be used to find scalar form factors [15] for charmonium mesons, along with energy shifts [16] and magnetic polarizabilities [16]. Thus we have reported some predictions about these quantities for conventional and hybrid charmonium mesons. We have also found the numerical values of square of radial wave functions at the origin ( $|R(0)|^2$ ), which can be used to calculate the decay constants [17], decay rates [17], and differential cross sections [18] for quarkonium states. The predictions about these quantities are also reported for conventional and hybrid charmonium mesons.

In the section II below, we write the Hamiltonian for the conventional mesons. Then we describe the shooting method-based numerical procedure to find the solution of the radial Schrödinger equation for conventional charmonium mesons. The expressions to find masses, root mean square radii, and squares of radial wave functions at the origin ( $|R(0)|^2$ ) of conventional charmonium mesons are also written in this section. In section III, the Hamiltonian is written for hybrid mesons, and then we redo all the numerical work as done in section II for hybrids now. The  $\chi^2$  and other error measures for different forms of the potential difference between ground and excited state are also written in section III. Results for the masses, root mean square radii and  $|R(0)|^2$  of conventional and hybrid mesons are reported in section IV for systems composed of charm quarks and antiquarks. Based on these results, we also include some results related to experimentally measurable quantities.

## II. Characteristics of Conventional charmonium mesons

### The Potential Model for Conventional Charmonium Mesons

In the potential models, the confining potential for  $Q\bar{Q}$  system in the the ground state gluonic field is mostly used in the form of

$$\frac{-4\alpha_s}{3r} + br + c, \quad (1)$$

with inter-quark distance  $r$ . Here,  $-4/3$  is due to the colour factor,  $\alpha_s$  is the quark-gluon coupling,  $b$  is the string tension and  $c$  is a constant. In above equation, the first term is due to one gluon exchange and the second term is the linear confining potential [19]. This potential form provides a good fit to the lattice simulations of refs. [20, 21, 22]. By including the Gaussian-smeared hyperfine interaction [23] and orbital angular momentum (or centrifugal) term, the potential of the  $Q\bar{Q}$  system for the ground state gluonic field have following form

$$V(r) = \frac{-4\alpha_s}{3r} + br + \frac{32\pi\alpha_s}{9m_c^2} \left(\frac{\sigma}{\sqrt{\pi}}\right)^3 e^{-\sigma^2 r^2} S_c \cdot S_{\bar{c}} + \frac{L(L+1)}{2\mu r^2}, \quad (2)$$

where  $S_c \cdot S_{\bar{c}} = \frac{S(S+1)}{2} - \frac{3}{4}$ ,  $\mu$  is the reduced mass of the quark and antiquark,  $m_c$  is the mass of the charm quark, and  $S$  is the total spin quantum number of the meson. For the  $c\bar{c}$  mesons, the parameters  $\alpha_s$ ,  $b$ ,  $\sigma$ , and  $m_c$  are taken to be 0.5461, 0.1425 GeV<sup>2</sup>, 1.0946 GeV and 1.4796 GeV respectively as in ref. [23]. The quantum numbers for the conventional charmonium mesons we choose for our study are reported below in Table 5.

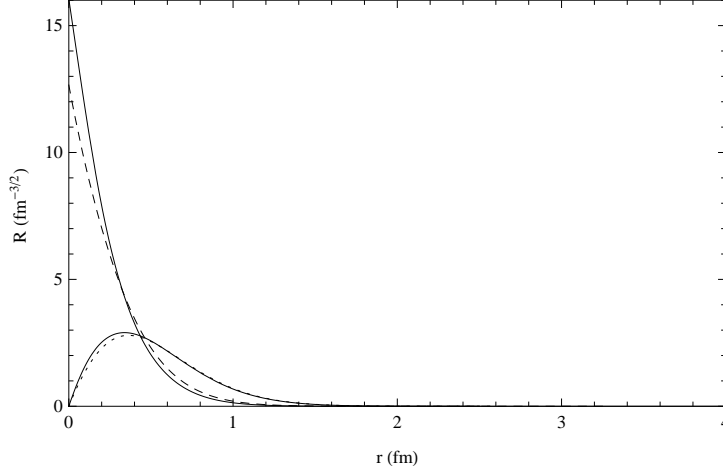


Figure 1: The radial parts of  $\eta, J/\psi, h_c,$  and  $\chi_c$  meson wave functions as functions of  $r$ . Thin solid line represents the  $\eta$  wave function, dashed line represents the  $J/\psi$  wave function, thick solid line represents the  $h_c$  wave function and points represent the  $\chi_c$  wave function.

## Wave Functions and Radii of Conventional Charmonium Mesons

A conventional meson can be described by the wave function of the bound quark-antiquark state which satisfies the Schrödinger equation with potential of eq.(2). Radial Schrödinger equation with wave function  $U(r) = rR(r)$  is written (in natural units) as

$$\frac{d^2}{dr^2}U(r) + 2\mu(E - V(r))U(r) = 0. \quad (3)$$

Here  $R(r)$  is the radial wave function,  $r$  is the interquark distance,  $E$  is the sum of kinetic and potential energy of quark-antiquark system, and  $V(r)$  and  $\mu$  are defined above through eq.(2).

In quark-antiquark bound state, the wave function must satisfy the boundary conditions  $U(0) = 0$  and  $U(\infty) = 0$ . For the numerical solution of the Schrödinger equation with the potential of eq.(2), we repeatedly generated energy  $E$  from -2 to 2 GeV in steps of 0.1 GeV. For each such trial initial energy, we used the Newton method [24] to select, if any, the energy for which the numerical solution of Schrödinger equation became zero at infinity. To obtain these numerical solutions, we used the RK method [25] with using any arbitrary integer value of  $U'(0)$ . For different values of  $U'(0)$ , normalized solutions of the Schrödinger equation, obtained by multiplying the solution with the normalization constant  $(\frac{1}{\sqrt{\int U^2(r)dr}})$ , remain the same. These energy eigenvalues plus constituent quark masses are taken to be the  $c\bar{c}$  mesons masses (in natural units). It is found that our results for conventional charmonium mesons agree with the Table 1 of ref. [23]. This supports the reliability of our method. We also checked the consistency of our method by 1) getting a 100% overlap of our  $HU$  and  $EU$  and 2) by calculating the masses of conventional mesons by the Crank Nicholson Discretization and finding that masses obtained by both of the methods are identical. The Fig.1 shows the dependence of  $\eta, J/\psi, h_c,$  and  $\chi_c$  normalized radial wave functions on the radial separation  $r$ . The quantum numbers ( $L$  and  $S$ ) for these particles are given below in Table 5. These graphs show that the radial wave functions of  $\eta, h_c, \chi_c,$  and  $J/\psi$  have the same properties as that of hydrogen atom radial wave functions, i.e. they behave as  $r^L$  for small inter quark distances and decrease exponentially at large inter quark distances. Thin solid and Dashed lines graphs are for  $L = 0$ , so these graphs are similar to  $r^0 \exp(-r)$ . Thick solid and points are for  $L = 1$ , so these graphs are similar to  $r^1 \exp(-r)$ . As  $L$  increases, the wave function's peak goes away from the origin. This means that centrifugal term has more effects on wave function than that of the hyperfine term. One possible reason is that we are dealing with heavy quarks so the  $1/m_c^2$  factor (shown in eq.(2)) of the hyperfine term becomes very small.

The normalized wave functions are used in the further calculations for root mean square radii and square of radial wave functions at origin. To find the root mean square radii of the  $c\bar{c}$  mesons, we used

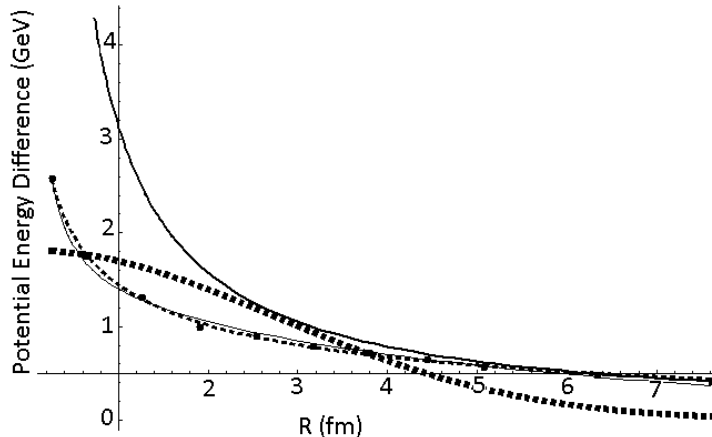


Figure 2: Graphs of potential energy differences between ground and excited state. Points represent the data taken from ref. [12], thick solid line represents potential difference model  $\frac{\pi}{r}$ , thin solid line represents the potential energy difference  $\frac{\pi}{r} + A \times \exp(-Br)$ , dashed line represents the potential difference  $A \times \exp(-Br^{0.1897})$ , and squared points represents the potential energy difference  $A \times \exp(-Br^2)$ .

the following relation:

$$\sqrt{\langle r^2 \rangle} = \sqrt{\int U^* r^2 U dr}. \quad (4)$$

In ref. [26], for normalized wave function

$$U'(0) = R(0) = \sqrt{4\pi} \psi(0) \quad (5)$$

is used and we use this prescription. Thus the derivative of  $U(r)$  at  $r = 0$  is calculated to find  $|R(0)|^2$ .  $|R(0)|^2$  is used in many applications of high energy physics as mentioned in section I.

### III. Characteristics of Hybrid Charmonium mesons

#### The Potential Model for Hybrid Charmonium Mesons

The centrifugal factor for the hybrid mesons is written in refs. [27, 28] as

$$\frac{L(L+1) - 2\Lambda^2 + \langle J_g^2 \rangle}{2\mu r^2} \quad (6)$$

where  $\Lambda$  is the projection of the total angular momentum  $J_g$  of the gluonic field. The states with  $\Lambda = 0, 1, 2, 3, \dots$  are usually represented by the capital greek letters  $\Sigma, \Pi, \Delta, \Phi, \dots$  respectively. We are interested in finding the masses and root mean square radii of the hybrid states  $0^{+-}, 1^{-+},$  and  $2^{+-}$ . These states can be generated from the  $\Pi_u$  potential. For the  $\Pi_u$  potential,  $\langle J_g^2 \rangle = 2$  and  $\Lambda = 1$  [28]. Therefore  $-2\Lambda^2 + \langle J_g^2 \rangle = 0$ , so centrifugal factor for the hybrid mesons is  $L(L+1)/2\mu r^2$ . In ref. [28]  $J = L \oplus S$ ,  $P = \epsilon(-1)^{L+\Lambda+1}$ , and  $C = \epsilon\eta(-1)^{L+\Lambda+S}$  with  $\epsilon, \eta = \pm 1$ . Therefore with same quantum numbers (L,S), different  $J^{PC}$  states are possible.  $L$  and  $S$  for these hybrid  $J^{PC}$  states are shown in Table 6 (as given in ref. [29]). For the excited part of quark antiquark potential  $\pi/r$  is used in the flux tube model [30]. This form of excitation energy is only valid at large inter-quark distances. In comparison, we suggest and evaluate excited potential energy in forms which are valid for smaller distances as well. For this purpose, we get the potential energy differences ( $\epsilon_i$ ) between ground and excited states for different  $r_i$  values from the lattice simulation reported in Fig. 3 of ref. [12], and calculate  $\chi^2$  with a variety ( $\pi/r$ ,  $A \times \exp(-Br^2)$ ,  $A \times \exp(-Br^{0.1897})$ ,  $\frac{\pi}{r} + A \times \exp(-Br^2)$ , and  $\frac{\pi}{r} + A \times \exp(-Br^{0.3723})$ ) of *ansatz* by fitting parameters appearing in each *ansatz*. Dimensionless  $\chi^2$  is defined as

$$\chi^2 = \frac{\sum_{i=1}^n (\epsilon_i - V_g(r_i))^2}{\sum_{i=1}^n \epsilon_i^2}, \quad (7)$$

Table 1: Our calculated  $\chi^2$  for the data of potential difference to our suggested models ( $V_g(r)$ ) with best fit parameter's values.

<i>ansatz</i>	$\chi^2$	$\chi^2/D$	$\chi$	Parameters			
				<i>A</i>	<i>B</i>	<i>c</i>	$\gamma$
		GeV <sup>2</sup>		GeV	GeV		
$\pi/r$	0.2305	0.3268	0.5285	-	-	-	-
$A \times \exp(-Br^2)$	0.0857	0.1215	0.2773	1.8139	0.0657	-	2
$A \times \exp(-Br^\gamma)$	0.0004	0.0005	0.0205	17.9325	2.5195	-	0.1897
$\frac{c}{r} + A \times \exp(-Br^\gamma)$	0.0012	0.0017	0.0331	1.2448	0.1771	0.3583	1
$\frac{c}{r} + A \times \exp(-Br^2)$	0.0003	0.0004	0.0132	3.4693	1.0110	0.1745	0.3723

with  $i = 1, 2, 3, \dots, n$  being number of data points. Here  $V_g(r)$  is a model of the potential energy difference between the ground and excited state. We tried

$$\begin{aligned}
 V_g(r) &= \pi/r, \\
 V_g(r) &= A \times \exp(-Br^2), \\
 V_g(r) &= A \times \exp(-Br^\gamma), \\
 V_g(r) &= \frac{c}{r} + A \times \exp(-Br), \\
 V_g(r) &= \frac{c}{r} + A \times \exp(-Br^\gamma).
 \end{aligned}
 \quad \text{and}$$

The parameters  $A, B, c$ , and  $\gamma$  are found by fitting these models ( $V_g(r)$ ) with the potential difference data of ref. [12], and reported in Table 1.  $\chi^2$ ,  $\chi^2/D$  and  $\chi$  are also reported in Tables 1 with  $\chi^2/D = \chi^2/(\text{Number of data points})$  and  $\chi = \frac{\sum_{i=1}^n |(\varepsilon_i - V_g(r))|}{\sum_{i=1}^n |\varepsilon_i|}$ .

It is noted that the  $\chi^2$  for  $\pi/r$  is greater than all other potential difference forms. Fig. 2, representing the graphs for different forms of potential difference, also shows the same behaviour. The  $\chi^2$  of the gaussian gluonic potential ( $A \times \exp(-Br^2)$ ) is less than  $\frac{\pi}{r}$ , but larger than all other forms.  $A \times \exp(-Br^2)$  is a smeared form of  $\frac{\text{constant}}{r}$ , as written in appendix of ref. [31]. The potential difference in this form ( $A \times \exp(-Br^2)$ ) has an advantage that it can be easily used in dynamical applications. For example, the expectation value of this part of the potential energy in a Gaussian wave function of the quadratic confining potential is given in terms of error function differences even if one uses antiderivatives to evaluate the definite integrals in it. Or, for usual infinite limits it simply multiplies in the integrand with already Gaussian meson wave functions to keep the integrand as Gaussian, whose well known integral can be written by inspection. (The expression for the expectation value can be minimized with respect to the chosen parameters of the wave function to find the ground state energy and wave function using the variational method.) This calculational advantage may be trivial for a two-body problem. But if one has to evaluate an expectation value for few or many body problem (or for a minor variant used in the resonating group method based treatment [32] [33] of a system of two quark and two antiquarks), we have to evaluate an integral of a high order whose direct numerical evaluation may have convergence problems as in ref. [33] and a Gaussian integration by inspection may well be the only practical option. The need to keep the multi-dimensional integrals as Gaussian, giving importance to the  $A \times \exp(-Br^2)$  form, becomes even more prominent when when wave functions of the conventional mesons are replaced for the respective problems by those of the hybrids as in ref. [32].

The analytic Gaussian expectation value of  $A \times \exp(-Br)$  term is similarly given in terms of error function differences. (Or, its product in integrand with Gaussian wave functions can be converted to a new Gaussian integrand using a completing of square.) The  $\chi^2$  for the potential difference in form of  $\frac{c}{r} + A \times \exp(-Br^{0.3723})$  is much less. The  $\frac{c}{r}$  term in this form can be used for analytical expressions of expectation values in the above mentioned Gaussian quark antiquark wave functions of quadratic potential, resulting in differences of the exponential integral functions for the most analytical way of finding the expectation values and integrals of resonating group method [32] [33]. But a similar fully analytical route for Gaussian expectation values and resonating group integrals of the  $A \times \exp(-Br^\gamma)$ , for  $\gamma = \text{non-integer number}$ , is not available, and this can lead to convergence problems [33] when we integrate numerically integrals of high dimensions.

In ref. [13], [28] excited state potential (*not* the difference) is used in the form of

$$c_0 + \sqrt{b_0 + b_1 r + b_2 r^2}. \quad (8)$$

Table 2: Our calculated  $\chi^2$  for the first excited state data of ref. [12] to the model used in ref. [13] with best fit parameter's values.

Excited Potential	$\chi^2$	$\chi^2/D$	$\chi$	Parameters			
				$b_0$	$b_1$	$b_2$	$c_0$
		GeV <sup>2</sup>		GeV <sup>2</sup>	GeV <sup>3</sup>	GeV <sup>4</sup>	GeV
$c_0 + \sqrt{b_0 + b_1 r + b_2 r^2}$	0.00096	0.0030	0.0226	58.0016	$4.4896 \times 10^{-10}$	0.2859	-6.1814

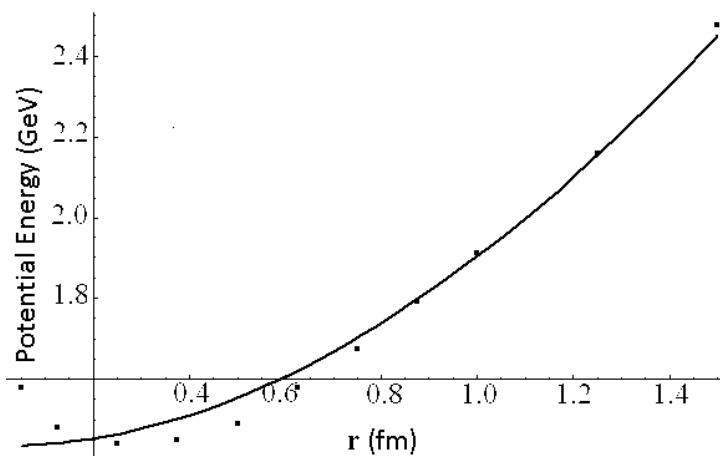


Figure 3: Graphs of excited state potential energy in the form of  $c_0 + \sqrt{b_0 + b_1 r + b_2 r^2}$  along with data of ref. [12]. Solid line is for the potential  $c_0 + \sqrt{b_0 + b_1 r + b_2 r^2}$  and dots are for data of ref. [12].

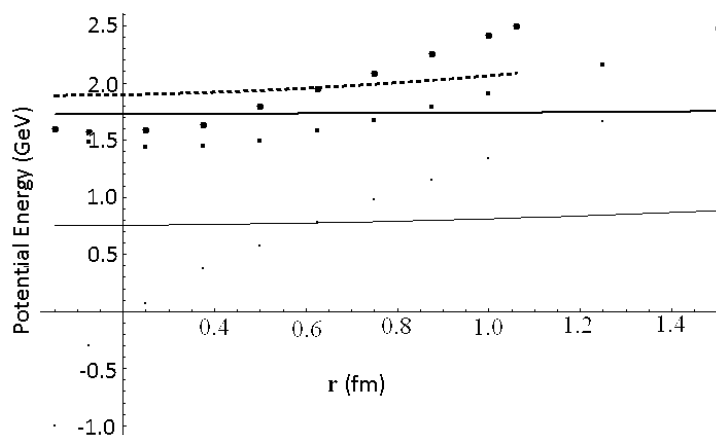


Figure 4: Graphs of potential energy in the form of  $\sqrt{\sigma^2 r^2 + 2\pi\sigma(N + \frac{3}{2})} + w_q$ . The solid line is for  $N = 0$  and small points are for  $N = 0$  data of ref. [12]. Thick solid line is for  $N = 1$  and medium size points are for  $N = 1$  data of ref. [12]. Dashed line is for the  $N = 2$  and large size points are for  $N = 2$  data of ref. [12].

Table 3: Our calculated  $\chi^2$  with best fit parameter's values.

<i>Excited Potential</i>	$\chi^2$	$\chi^2/D$	$\chi$	$N$	Parameters	
					$w_q$	$\sigma$
		GeV <sup>2</sup>	GeV	-	GeV <sup>2</sup>	GeV <sup>4</sup>
	0.5536	0.6633	0.6932	0	$5.9884 \times 10^{-9}$	0.0601
$\sqrt{\sigma^2 r^2 + 2\pi\sigma(N + \frac{3}{2})} + w_q$	0.0112	0.0348	0.0899	1	$3.5044 \times 10^{-7}$	0.1629
	0.0190	0.0740	0.1259	2	$1.0531 \times 10^{-5}$	0.1627

By fitting this potential with data of first excited potential taken from Fig.3 of ref. [12], we calculated the parameters  $b_0, b_1, b_2, c_0$ . We also calculated  $\chi^2, \chi$  and  $\chi^2/D$  and reported in Table 2 along with the parameter values. The fit of the data with this excited state potential is shown in our Fig.3. As for the analytical calculations (for finding expectation values etc.), these are also not possible with this potential form and thus for many applications it has to be replaced by others of higher chisquare.

Fig.4 shows the behaviour of string potential [34]

$$\sqrt{\sigma^2 r^2 + 2\pi\sigma(N + \frac{3}{2})} + w_q \quad (9)$$

with  $N = 0, 1, 2$ . In this figure, the points represent the data taken from ref. [12]. The parameter's values,  $\chi^2$  and other error measures of the string potential with the data (of excited potential) of ref. [12] is reported in Table 3. The parameter's values are calculated by fitting the data of excited potential with the string potential. The analytical calculations (for finding expectation values) are not possible with this string potential form as well.

## Wave Functions and Radii of Hybrid Charmonium Mesons

Now, we can write the quark antiquark potential in excited state gluonic field as

$$V(r) = \frac{-4\alpha_s}{3r} + br + \frac{32\pi\alpha_s}{9m_c^2} \left(\frac{\sigma}{\sqrt{\pi}}\right)^3 e^{-\sigma^2 r^2} S_c \cdot S_{\bar{c}} + \frac{L(L+1) - 2\Lambda^2 + \langle J_g^2 \rangle}{2\mu r^2} + V_g(r). \quad (10)$$

$V_g(r)$  is defined above after eq.(7).

Using this excited state potential of eq.(10) along with the above mentioned values (after eq.(6)) of  $\Lambda$  and  $\langle J_g^2 \rangle$ , the energy eigenvalues and the corresponding wave functions are found by using the same technique as employed for conventional mesons (mentioned in section II). As before, these eigenvalues plus constituent quark antiquark masses are taken to be the masses of hybrid mesons. Then we normalized the wave functions and found the root mean square radii of hybrid mesons by using eq.(4). The normalized radial wave functions for charmonium hybrid mesons are graphically represented in Fig.5 and Fig.6. The overlaps of our numerically calculated radial wave functions ( $U = rR$ ) for the excited states and a modified gaussian wave function ansatz

$$\psi = n r^2 \exp(-pr^2) \quad (11)$$

multiplied by  $\sqrt{4\pi r}$  are written in Table 4 in such a way that  $U = rR = \sqrt{4\pi r}\psi$ .

The normalization of the gaussian wave function gives

$$n = (42^{\frac{3}{4}} p^{\frac{7}{4}}) (15^{\frac{1}{2}} \pi^{\frac{3}{4}}). \quad (12)$$

The numerical value of  $p$  is found by fitting this function with the data of numerically calculated wave function, and written in Table 4.

The Fig.5 and Fig.6 show the wave function dependence on  $L$  and  $S$ . Therefore the masses and root mean square radii of  $0^{+-}, 1^{-+}$  and  $2^{+-}$   $J^{PC}$  states also depend on the quantum numbers  $L$  and  $S$ .  $|R(0)|^2$  is found for hybrid mesons using eq.(5). The Fig.5 and Fig.6 also show that the peaks of the graphs for radial probability density are in agreement with the peak of radial probability curve drawn in ref. [12].

Table 4: Our best fit parameter's values and overlaps of numerically solved wave functions to the wave function form written in eq.(11).

<i>ansatz</i>	$L = 1$ and $S = 1$			$L = 2$ and $S = 1$		
	Parameters of excited state function written in eq.(11)		Overlap	Parameters of excited state function written in eq.(11)		Overlap
	$n$	$p$		$n$	$p$	
$\pi/r$	0.0047	0.0556	0.9997	0.0032	0.0451	0.9989
$A \times \exp(-Br^2)$	0.0031	0.0439	0.9964	0.0025	0.0391	0.9905
$A \times \exp(-Br^{0.1897})$	0.0093	0.0822	0.9903	0.0048	0.0565	0.9998
$\frac{c}{r} + A \times \exp(-Br)$	0.0070	0.0698	0.9899	0.0036	0.0482	0.9999
$\frac{c}{r} + A \times \exp(-Br^{0.3723})$	0.0087	0.0794	0.9903	0.0045	0.0547	0.9998
$c_0 + \sqrt{b_0 + b_1r + b_2r^2}$	0.0163	0.1135	0.9921	0.0090	0.0807	0.9999

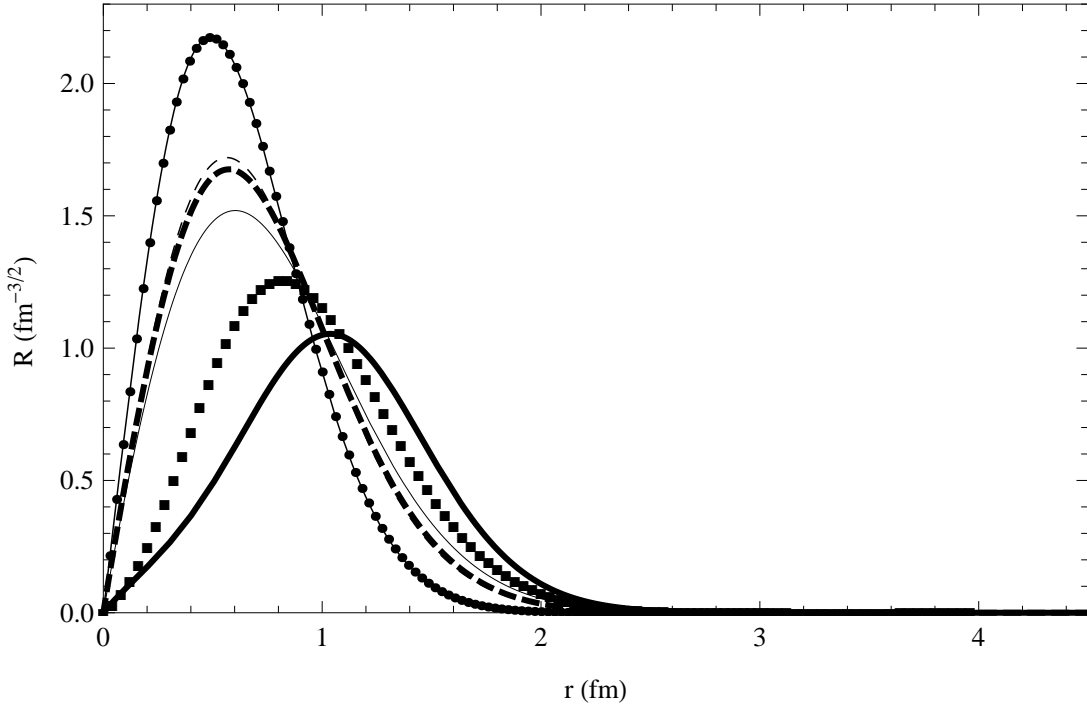


Figure 5: Hybrid charmonium meson radial wave functions for  $0^{+-}$ ,  $1^{-+}$  and  $2^{+-}$   $J^{PC}$  states for  $L=1$  and  $S=1$ . The wave function with potential in the form of coulombic plus linear plus  $A \exp(-Br^2)$  is represented by the solid line. Wave function with coulombic plus linear plus  $\pi/r$  potential is represented by square points. Wave function with coulombic plus linear plus  $A \times \text{Exp}(-B r^{0.1896})$  potential is represented by dashed line. Wave function with coulombic plus linear plus  $\frac{c}{r} + A \times \text{Exp}(-B r)$  potential is represented by thin solid line. Wave function with coulombic plus linear plus  $\frac{c}{r} + A \times \text{Exp}(-B r^{0.3723})$  potential is represented by thick dashed line, and the wave function with excited potential in the form of  $c_0 + \sqrt{b_0 + b_1r + b_2r^2}$  is represented by points with lines.



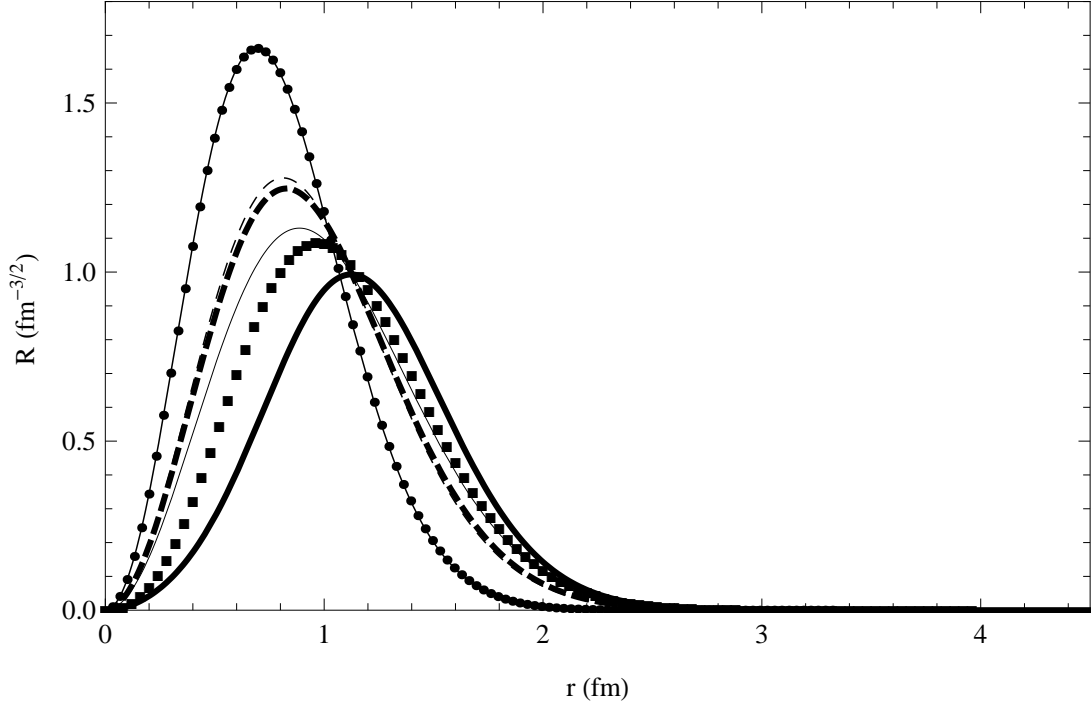


Figure 6: The same figure as Fig.4 but with  $L = 2$  and  $S = 1$ .

## IV. Results and Conclusions

1. For conventional mesons, our calculated masses and root mean square radii are reported in Table 5 along with the experimental and theoretical predictions of the other works. We observed that our results are in good agreement with the experimental and existing theoretically predicted values, which shows the validity of our method. Quantum mechanically, when  $L$  increases, centrifugal barrier increases so particles become less bound implying increased root mean square radii. Our calculated root mean square radii are in agreement with this expectation.

2. With the parameters (given in Table 6) for the  $0^{+-}, 1^{-+}$  and  $2^{+-}$   $J^{PC}$  states, masses and root mean square radii are calculated for the charmonium hybrid mesons. In Table 6, masses are calculated using the excited state gluonic field potential in the above mentioned forms. For comparison with earlier works, masses of  $c\bar{c}$  hybrid mesons with  $0^{+-}, 1^{-+}$  and  $2^{+-}$   $J^{PC}$  states are given in Table 7. In Table 8, root mean square radii are calculated by taking the excited state potential in the coulomb plus linear plus additional excited potential. In Table 9, masses and root mean square radii are reported for the excited potential in the form of  $c_0 + \sqrt{b_0 + b_1 r + b_2 r^2}$ .

3. For conventional mesons  $|R(0)|^2$  is reported in Table 10. Each  $|R(0)|^2$  of  $c\bar{c}$  hybrid mesons for  $0^{+-}, 1^{-+}$  and  $2^{+-}$   $J^{PC}$  states is equal to zero by our calculation and this result agrees with ref. [37] which writes "models of hybrids typically expect the wave function at the origin to vanish". We also noted that the masses and root mean square radii of the hybrid mesons are greater than ordinary mesons with the same flavour and quantum numbers ( $L$  and  $S$ ). Since  $0^{+-}, 1^{-+}, 2^{+-}$  states are not possible with quark model quantum numbers, so we can not compare these  $J^{PC}$  states with conventional mesons.

In ref. [15], the scalar form factor is written as

$$\bar{\Gamma}_\pi(t) = 1 + \frac{1}{6} \langle r^2 \rangle_s t + o(t^2). \quad (13)$$

In ref. [16], energy shift and magnetic polarizability are written as

$$\Delta E_n = \langle n | \frac{eH}{8\mu} L_3 + \left( \frac{e^2}{4\tilde{\mu}} + \frac{q^2}{\mu_1 + \mu_2} \right) \frac{H^2 r^2 \sin^2 \theta}{32} | n' \rangle + \Sigma'_n \frac{|\langle n' | eHL_3/8\tilde{\mu} | n \rangle|^2}{E_n - E_{n'}}. \quad (14)$$

Here the symbol  $L_3, H, e, m$  are used for the angular momentum, magnetic field, charge and mass of the quark,  $\tilde{\mu} = \frac{\mu}{2}$ ,  $\theta$  is the angle between  $H$  and relative co-ordinate  $r$ ,  $q = e_1 - e_2$ , and  $e = e_1 + e_2$ . In above

Table 5: The experimental and theoretical masses and theoretical root mean square radii of some conventional charmonium mesons. The experimental mass is the average PDG [23] and rounded to 0.001 GeV. Our calculated masses are rounded to 0.0001 GeV.

Meson	$L$	$S$	Our calculated mass	Theor. mass [23] with NR potential model	Exp. mass	our calculated $\sqrt{\langle r^2 \rangle}$	Theor. $\sqrt{\langle r^2 \rangle}$ [35] with potential model
			GeV	GeV	GeV	fm	fm
$\eta_c$	0	0	2.9816	2.982	$2.9792 \pm 0.0013$ [23]	0.365	0.388
$J/\psi$	0	1	3.0900	3.090	$3.09687 \pm 0.00004$ [23]	0.414	0.404
$h_c$	1	0	3.5156	3.516	$3.525 \pm 0.00055$ [23]	0.674	0.602
$\chi_c$	1	1	3.5246	3.556	$3.55618 \pm 0.00013$ [36]	0.685	0.606

Table 6: Our calculated masses of  $c\bar{c}$  hybrid meson  $0^{+-}, 1^{-+}$  and  $2^{+-}$   $J^{PC}$  states.

$J^{PC}$	$L$	$S$	$\Lambda$	$\langle J_q^2 \rangle$	Excited potential as coulombic plus linear plus				
					$\pi/r$	$A \times \exp(-Br^2)$	$A \times \exp(-Br^{0.1897})$	$\frac{c}{r} + A \times \exp(-Br)$	$\frac{c}{r} + A \times \exp(-Br^{0.3723})$
					GeV	GeV	GeV	GeV	GeV
$0^{+-}, 1^{-+}, 2^{+-}$	1	1	1	2	4.3571	4.0619	4.2680	4.2733	4.2694
$1^{-+}, 2^{+-}$	2	1	1	2	4.4632	4.1433	4.4632	4.4258	4.40796

Table 7: The mass predictions of  $1^{-+}, 0^{+-}$  and  $2^{+-}$  states of other works.

Predicted masses (GeV)			models
$1^{-+}$	$0^{+-}$	$2^{+-}$	
$\approx 3.9$ [38]			bag model
4.2-4.5 [39]-[41]			flux tube model
$4.19 \pm sys.error$ [42] [43]	$\approx 4.5$ [13]	$\approx 4$ [13]	heavy quark LGT
4.7 [44]	4.58 [44]		
4.1-4.5			QCD sum rules
4.369 – 4.420 [45, 46, 47]	4.714(52) [47]	4.895(88) [48]	quenched lattice QCD

Table 8: Our calculated root mean square radii of  $c\bar{c}$  hybrid meson  $0^{+-}, 1^{-+}$  and  $2^{+-}$   $J^{PC}$  states.

$J^{PC}$	$L$	$S$	$\Lambda$	$\langle J_q^2 \rangle$	$\sqrt{\langle r^2 \rangle}$ with excited potential as coulombic plus linear plus				
					$\pi/r$	$A \times \exp(-Br^2)$	$A \times \exp(-Br^{0.1897})$	$\frac{c}{r} + A \times \exp(-Br)$	$\frac{c}{r} + A \times \exp(-Br^{0.3723})$
					fm	fm	fm	fm	fm
$0^{+-}, 1^{-+}, 2^{+-}$	1	1	1	2	1.1061	1.2458	0.9110	0.9881	0.9272
$1^{-+}, 2^{+-}$	2	1	1	2	1.2280	1.3203	1.0988	1.1883	1.1160

Table 9: Our calculated masses and root mean square radii with excited potential  $c_0 + \sqrt{b_0 + b_1 r + b_2 r^2}$  of  $c\bar{c}$  hybrid meson with  $0^{+-}, 1^{-+}, 2^{+-}$   $J^{PC}$  states.

$J^{PC}$	$L$	$S$	$\Lambda$	$\langle J_g^2 \rangle$	masses GeV	$\sqrt{\langle r^2 \rangle}$ fm
$0^{+-}, 1^{-+}, 2^{+-}$	1	1	1	2	4.9503	0.7748
$1^{-+}, 2^{+-}$	2	1	1	2	5.1693	0.9185

Table 10:  $|R(0)|^2$  of  $c\bar{c}$  meson

Meson	$L$	$S$	our calculated normalized $ R(0) ^2$ $GeV^3$
$\eta$	0	0	1.2294
$J/\psi$	0	1	1.9767
$h_c$	1	0	$\approx 0$
$\chi_c$	1	1	$\approx 0$

equation, the term having  $\langle n | \frac{H^2 r^2 \sin^2 \theta}{32} | n' \rangle$  is related to square of root mean square radii.

$$\beta = -\frac{1}{24} \left( \frac{e^2}{4\tilde{\mu}} + \frac{q^2}{\mu_1 + \mu_2} \right) \langle r^2 \rangle. \quad (15)$$

In above eqs.(13-15) the root mean square radii is in the numerator, therefore we predict that magnitudes of scalar form factor [15], energy shift [16], and magnetic polarizability [16] for hybrids are greater than those for conventional mesons of the same quantum numbers ( $L$  and  $S$ ).

By parametrizing the excited state wave function written above in eq.(11), we get

$$\langle r^2 \rangle = \int \psi^* r^2 \psi dr = \frac{15n^2 \sqrt{\pi/2}}{128p^{7/2}}. \quad (16)$$

Here  $n$  is a function of  $p$ , as given by eq.(12). Substituting the result of eq.(16) in eqs.(13,15), the scalar form factor and magnetic polarizability become

$$\bar{\Gamma}_\pi(t) = 1 + \frac{1}{6} \frac{15n^2 \sqrt{\pi/2}}{128p^{7/2}} t + o(t^2), \quad (17)$$

$$\beta = -\frac{1}{24} \left( \frac{e^2}{4\tilde{\mu}} + \frac{q^2}{\mu_1 + \mu_2} \right) \frac{15n^2 \sqrt{\pi/2}}{128p^{7/2}}. \quad (18)$$

Numerically calculated values of  $n$  and  $p$  are written in Table 4 for different forms of excited state potentials for different  $L$  and  $S$ .

As we mentioned above,  $|R(0)|^2$  is equal to zero for hybrid mesons. Using this result, we can predict that decay constants [17], decay rates [17], and differential cross sections [18] of hybrid mesons are zero as these quantities are proportional to  $|R(0)|^2$  as written in these references.

## Acknowledgement

We are grateful to Higher education Commission of Pakistan for their financial support no.17-5-3 (Ps3-212) HEC/Sch/2006.

## References

- [1] C. McNeile, Nucl. Phys. A **711**, 303 (2002).

- [2] The COMPASS Collaboration (M. Alekseev et al.), Phys. Rev. Lett. **104**, 241803 (2010) The COMPASS Collaboration (B. Grube et al.), arXiv:1002.1272 [hep-ex] (2010).
- [3] VES Collaboration (Yu. P. Gouz et al.), AIP Conf. Proc. **272**, 572 (1993)
- [4] VES Collaboration (Yu A.Khokholov et al.), Nucl. Phys. A **663**, 596 (2000)
- [5] VES Collaboration (A. Zaitsev et al.), Nucl. Phys. A **675**, 155c (2000).
- [6] E852 Collaboration (G. S. Adams et al.), Phys. Rev. Lett. **81**, 5760 (1998).
- [7] E852 Collaboration (S. U. Chung et al.), Phys. Rev. **D65**, 072001 (2002).
- [8] E. I. Ivanov et al. [E852 Collaboration], Phys. Rev. Lett. **86**, 3977 (2001).
- [9] J. Kuhnel et al. [E852 Collaboration], Phys. Lett. **B 595**, 109 (2004).
- [10] M. Luetal. [E852 Collaboration], Phys. Rev. Lett. **94**, 032002 (2005).
- [11] C. A. Baker et al., Phys. Lett. **B563**, 140 (2003).
- [12] K. J. Juge, J. Kuti and C. Morningstar, AIP Conf. Proc. **688**, 193 (2003).
- [13] C. J. Morningstar and M. Peardon, Phys. Rev. **D 56**, 4043 (1997).
- [14] S. Collins, C. T. H. Davies, G. Bali, Nucl. Phys. Proc. Suppl. **63**, 335 (1998).
- [15] B. Ananthanarayan, I. Caprini, G. Colangelo, J. Gasser and H. Leutwyler, Phys. Lett. **B 602**, 218 (2004).
- [16] S. I. Kruglov, Phys. Rev. **D 60**, 116009 (1999).
- [17] B. Patel and P. C. Vinodkumar, J. Phys. **G 36**, 035003 (2009).
- [18] C. H. Chang, C. F. Qiao, J. X. Wang, Phys. Rev. **D 57**, 4035 (1998).
- [19] D. H. Perkins, *Introduction to High Energy Physics*, Addison-Wesley (1987).
- [20] Bali G S et al. , Phys. Rev **D62**, 054503 (2000).
- [21] Bali G S, Phys. Rep. **343**, 1 (2001).
- [22] Alexandrou C, de Forcrand P and John O, Nucl. Phys. **B119**, 667 (2003).
- [23] T. Barnes, S. Godfrey, and E. S. Swanson, Phys. Rev. **D 72**, 054026 (2005).
- [24] C. F. Gerald and P. O. Wheatley, *Applied Numerical Method*, published by Dorling Kindersley Pvt. Ltd., (1999).
- [25] Dr. V. N. Vedamurthy and Dr. N. Ch. Sniyengar, *Applied Numerical Methods*, Published by Vikas publishing House Pvt. Ltd., (1998).
- [26] M. M. Feyli, Proceedings of World Academy of Science, Engineering and Technology **71**, 565 (2010).
- [27] K. J. Juge, J. Kuti, and C. J. Morningstar, Phys. Rev. Lett., **82**, 4400 (1999).
- [28] K. J. Juge, J. Kuti and C. J. Morningstar, Nucl. Phys. Proc. Suppl. **63**, 326 (1998).
- [29] E. S. Swanson, talk presented at JLAB/INT Workshop on Gluonic Excitations, Newport News, Virginia, arXiv:hep-ph/ 0311328 (2003).
- [30] N. Isgur and J. Paton, Phys. Rev. **D 31** 2910 (1985).
- [31] J. Weinstein and N. Isgur, Phy. Rev. **D 41**, 2236 (1990).
- [32] N. Akbar and B. Masud, arXiv: 1102.1690 (2011).
- [33] M. I. Jamil and B. Masud, Eur. Phys. Jour. **A 47** (2011).

- [34] F. Buissereta, V. Mathieua, C. Semaya, and B. Silvestre-Brac, *Eur. Phys. J. A* ,**32**, 123 (2007).
- [35] Cheuk-Yin Wong, E. S. Swanson, and T. Barnes, *Phys. Rev. C* **65**, 014903 (2002).
- [36] K. K. Seth, *Jour. Phys. Conf. Ser.* **9**, 32 (2005).
- [37] S. Godfrey, Flavor Physics and CP Violation Conference, Vancouver, ECONF C 060409: 015, arXive: hep-ph/0605152 (2006).
- [38] P. Hasenfratz, R. R. Horgan, J. Kuti and J. M. Richard, *Phys. Lett. B* **95**, 299 (1980).
- [39] J. Merlin and J. Paton, *J. Phys. G* **11**, 439 (1985).
- [40] N. Isgur and J. Paton, *Phys. Rev. D* **31**, 2910 (1985).
- [41] J. Merlin and J. Paton, *Phys. Rev. D* **35**, 1668 (1987).
- [42] L. A. Griffiths, C. Michael, and P. E. L. Rakow, *Phys. Lett. B* **129**, 351 (1983).
- [43] S. Perantonis and C. Michael *Nucl. Phys. B* **347**, 854 (1990).
- [44] F. Iddir and L. Semlala, arXive hep-ph/0611165v2 (2006).
- [45] T. Mankeetal., *Phys. Rev. Lett.***82**, 4396 (1999).
- [46] Z. H. MeianX., Q. Luo, *Int. J. Mod. Phys. A* **18**,5713 (2003).
- [47] Y. Liu and X. Q. Luo, *Phys. Rev. D* **73**, 054510 (2006).
- [48] X. Liu, T. Manke, arXive:hep-lat/0210030.